Journal of Power Sources 217 (2012) 491–497

Contents lists available at SciVerse ScienceDirect

Journal of Power Sources

journal homepage: www.elsevier.com/locate/jpowsour

Short communication

Electrochemical performance of $LiNi_{1/3}Co_{1/3}Mn_{1/3}O_2$ thin film electrodes prepared by pulsed laser deposition

Jianqiu Deng [a,*], Liujiang Xi [b], Lihua Wang [c], Zhongmin Wang [a], C.Y. Chung [b], Xiaodong Han [c], Huaiying Zhou [a]

[a] School of Material Science and Engineering, Guilin University of Electronic Technology, Guilin 541004, China
[b] Department of Physics & Materials Science, City University of Hong Kong, Tat Chee Avenue, Kowloon, Hong Kong SAR, China
[c] Institute of Microstructure and Property of Advanced Materials, Beijing University of Technology, Beijing 100022, China

HIGHLIGHTS

- $LiNi_{1/3}Co_{1/3}Mn_{1/3}O_2$ thin films are successfully prepared by PLD technique.
- The optimal deposition time and annealing temperature are 30 min and 450 °C.
- The initial discharge capacity is 177 mAh g^{-1} tested at a rate of 0.1C.
- The Li-ion diffusion coefficients are in the range of 10^{-9}–10^{-10} cm^2 s^{-1}.

ARTICLE INFO

Article history:
Received 18 April 2012
Received in revised form
30 May 2012
Accepted 1 June 2012
Available online 16 June 2012

Keywords:
Thin film electrode
Lithium ion batteries
Electrochemical performance
Pulse laser deposition

ABSTRACT

Layered $LiNi_{1/3}Co_{1/3}Mn_{1/3}O_2$ thin film electrodes are successfully prepared by pulsed laser deposition technique and post-annealed. The microstructure of the thin films is characterized by X-ray diffraction, field emission scanning electron microscopy, X-ray photoelectron spectroscopy and transmission electron microscopy. The electrochemical performance of the thin film electrodes is evaluated by cyclic voltammetry and galvanostatic charge–discharge measurements. The kinetics of Li diffusion in the thin film electrodes are investigated by galvanostatic intermittent titration technique. The annealed thin films exhibit a partially amorphous structure. The electrochemical performance of $LiNi_{1/3}Co_{1/3}Mn_{1/3}O_2$ thin film electrodes depends on the annealing temperature, composition and thickness. The thin film electrodes deposited for 30 min with the annealing temperature of 450 °C deliver the best electrochemical performance, including high capacities, good cycle performance and rate capability. The initial discharge capacity of the thin film electrodes is 177 mAh g^{-1} measured at a rate of 0.1C in the voltage range of 2.8–4.5 V. The capacity retention ratio is 92% after 25 cycles at 0.5C rate. The chemical diffusion coefficients of lithium ion in the thin film electrodes are in the range of 10^{-9}–10^{-10} cm^2 s^{-1}.

1. Introduction

The cathode material most commonly used in the current commercial lithium ion batteries is the layered oxide $LiCoO_2$ because of its high theoretical capacity (274 mAh g^{-1}), good cycling stability and rate capability [1,2]. However, some drawbacks of $LiCoO_2$ such as the low practical capacity, the high cost, the safety problems and performance degradation during overcharging limit its further use in large-scale applications [3–5].

$LiNi_{1/3}Co_{1/3}Mn_{1/3}O_2$, a derivative of $LiCoO_2$, has been reported as a promising cathode material to replace $LiCoO_2$ [6]. It shows excellent electrochemical performance and intriguing structural behavior. $LiNi_{1/3}Co_{1/3}Mn_{1/3}O_2$ has the same structure as $LiCoO_2$ (α-$NaFeO_2$ structure), and the valence states of Ni, Co and Mn are 2^+, 3^+, and 4^+, respectively [7]. A small amount of cation disorder, as well as a small volume change, is observed in $LiNi_{1/3}Co_{1/3}Mn_{1/3}O_2$ during the charge/discharge process [8,9]. In addition, $LiNi_{1/3}Co_{1/3}Mn_{1/3}O_2$ presents excellent safety properties at a relatively high temperature (55 °C) [10]. Recently, researchers still focus on the study of $LiNi_{1/3}Co_{1/3}Mn_{1/3}O_2$ powders [11–13]. Nevertheless, the only study on $LiNi_{1/3}Co_{1/3}Mn_{1/3}O_2$ thin films has been reported by Xie et al. when our study is under way [14]. Unfortunately, the cycle performance of the $LiNi_{1/3}Co_{1/3}Mn_{1/3}O_2$ thin film electrodes prepared by RF magnetron sputtering is not obtained.

In this study, $LiNi_{1/3}Co_{1/3}Mn_{1/3}O_2$ thin films were successfully prepared by pulsed laser deposition (PLD) technique. The

* Corresponding author. Tel./fax: +86 773 2291434.
E-mail address: jqdeng@guet.edu.cn (J. Deng).

0378-7753/$ – see front matter © 2012 Elsevier B.V. All rights reserved.
http://dx.doi.org/10.1016/j.jpowsour.2012.06.006

electrochemical performance of $LiNi_{1/3}Co_{1/3}Mn_{1/3}O_2$ thin film electrodes was investigated in details. Furthermore, the effects of the annealing temperature, composition and thickness on the electrochemical performance of thin film electrodes were also discussed.

2. Experimental

The $LiNi_{1/3}Co_{1/3}Mn_{1/3}O_2$ powders were synthesized by hydroxide co-precipitation. The target was prepared by using $LiNi_{1/3}Co_{1/3}Mn_{1/3}O_2$ powders with 15 mol% Li_2O to compensate for Li loss during the deposition and heat treatment processes of thin films. $LiNi_{1/3}Co_{1/3}Mn_{1/3}O_2$ thin films were deposited on Pt/Ti/SiO_2/Si substrates at ambient temperature in an O_2 atmosphere of 50 mTorr for different time by PLD technique using a KrF excimer laser (Lambda Physik LPX 200). The thicknesses of Pt current collector layer and Ti buffer layer were 150 nm and 100 nm, respectively. The as prepared thin films were then annealed at 400, 450 and 500 °C for 3 h in air to improve crystallization. The microstructure of $LiNi_{1/3}Co_{1/3}Mn_{1/3}O_2$ thin films was characterized by X-ray diffraction (XRD), X-ray photoelectron spectroscopy (XPS) field emission scanning electron microscopy (FE-SEM) and transmission electron microscopy (TEM).

A two-electrode cell test equipment with lithium metal foil as the counter electrode was used in the galvanostatic charge–discharge tests, conducting by an Arbin BT-2000 battery testing system. A three-electrode cell test equipment was used in cyclic voltammetry (CV) and galvanostatic intermittent titration technique (GITT) measurements. CV measurements were carried out by using a Zaher Elektrik IM6 electrochemical workstation between 2.8 V and 4.5 V versus Li/Li^+ at different sweep rates. For GITT measurements, the cell was charged for 30 min at a current density of 1 μA cm^{-2} followed by an open circuit relaxation of 1 h. All experiments were performed in an Ar-filled glove box. One mole $LiClO_4$ in propylene carbonate (PC) was used as the electrolyte.

3. Results and discussion

3.1. Structure and morphology analysis of $LiNi_{1/3}Co_{1/3}Mn_{1/3}O_2$ thin films

The X-ray diffraction pattern of the $LiNi_{1/3}Co_{1/3}Mn_{1/3}O_2$ target with 15% excess Li_2O is shown in Fig. 1a. All the diffraction peaks can be indexed to a hexagonal α-$NaFeO_2$-type layered structure belonging to the R3m space group [15], without the appearance of any unknown diffraction peak. The XRD pattern of the $LiNi_{1/3}Co_{1/3}Mn_{1/3}O_2$ thin films annealed at low temperature (T = 400 °C) exhibits only the diffraction peaks of the substrate, indicating amorphous structure of thin films. The crystalline phase appears upon increasing the annealing temperature ($T \geq 450$ °C). The XRD pattern of the $LiNi_{1/3}Co_{1/3}Mn_{1/3}O_2$ thin films annealed at 500 °C (see Fig. 1b) displays a dominant peak at about 18.7°, which is attributed to the plane (003) reflection. The slightly intensive dominant peak indicates that the annealed thin films possess a partially amorphous structure.

In order to confirm the partially amorphous structure of the annealed thin films, TEM analysis was conducted. Fig. 2 (a, b) shows the TEM image and the selection area electron diffraction (SAED) pattern of the thin film annealed at 500 °C. The thin film was deposited on Si substrate for 90 min. From the cross-section TEM image, the thickness of thin film is about 400 nm and the growth rate is about 4.4 nm min^{-1}. The grain size is about from 10 nm to 200 nm. The diffusive diffraction rings are visible in the SAED pattern, which indicates that the amorphous structure exists in the thin film. *High-resolution transmission electron microscopy* (*HRTEM*) was also performed to examine the crystallinity of the thin film. The area marked by red circle in Fig. 2c shows an apparently amorphous region.

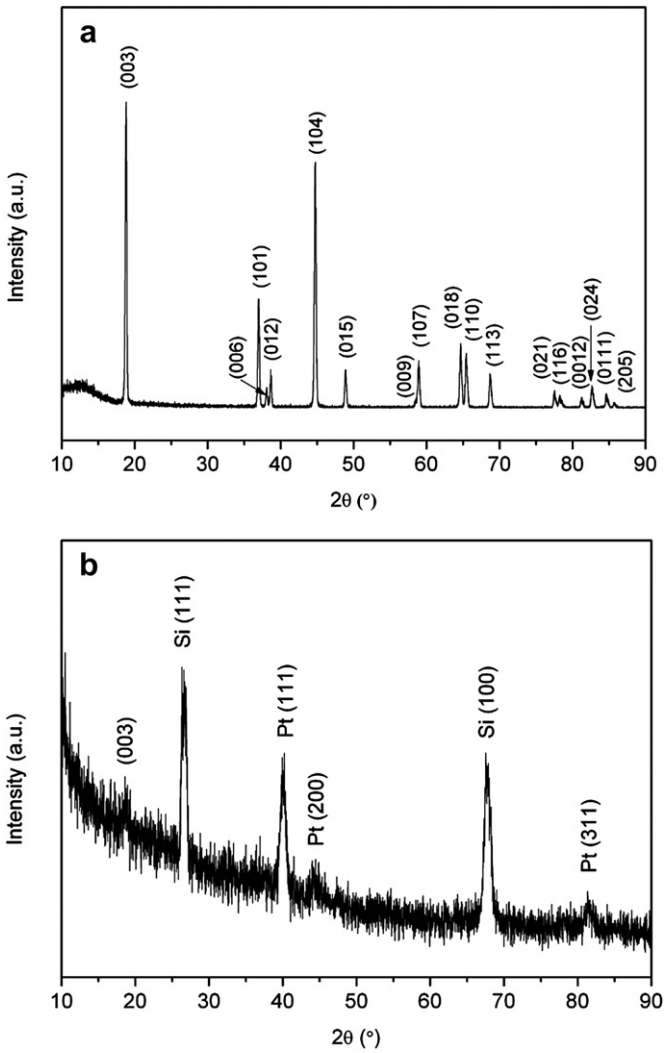

Fig. 1. XRD patterns of the $LiNi_{1/3}Co_{1/3}Mn_{1/3}O_2$ target and the thin film annealed at 500 °C for 3 h in air: (a) target, (b) thin film deposited for 30 min.

The FE-SEM images of $LiNi_{1/3}Co_{1/3}Mn_{1/3}O_2$ thin films annealed at various temperatures with deposition time of 30 min are shown in Fig. 3. The surface of the thin film annealed at 400 °C is smooth with an average grain size of about 15 nm (The surface image is not displayed in Fig. 3). The surface becomes rougher, and the grains grow bigger with increasing annealing temperature. The average grain size is about 20 nm and 30 nm for the thin films annealed at 450 °C (Fig. 3a) and 500 °C, respectively. The increasing surface roughness of the thin films with the increase of annealing temperature is also observed from the cross-section FE-SEM images (Fig. 3b–d). All the thin films show the columnar structure. The thicknesses of thin films annealed at 400, 450 and 500 °C are estimated to be about 105, 110 and 120 nm, respectively.

3.2. XPS analysis of $LiNi_{1/3}Co_{1/3}Mn_{1/3}O_2$ thin films

Prior to collecting the XPS data, the surface (about 20 nm thickness) of $LiNi_{1/3}Co_{1/3}Mn_{1/3}O_2$ thin films was etched by ion beam sputtering to remove any surface contaminations. The Ni2p, Co2p and Mn2p spectra of the $LiNi_{1/3}Co_{1/3}Mn_{1/3}O_2$ thin film

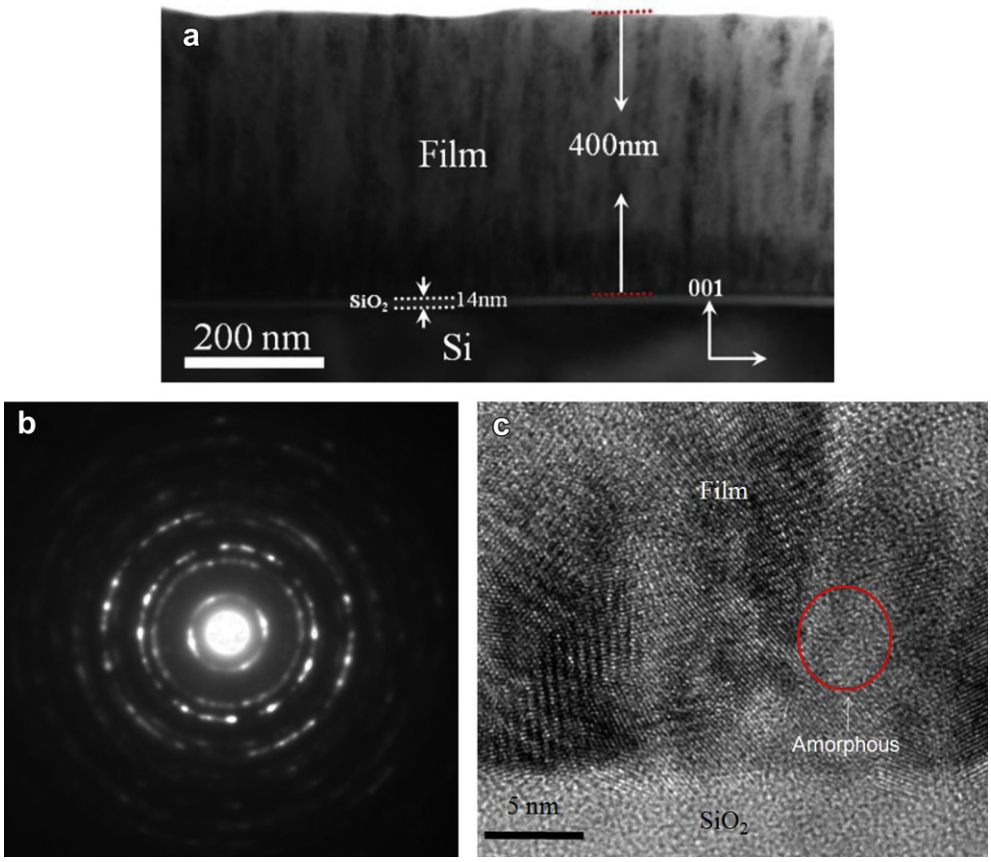

Fig. 2. The TEM image (a), the selection area electron diffraction (SAED) pattern (b) and HRTEM image (c) of the thin film deposited for 90 min and annealed at 500 °C.

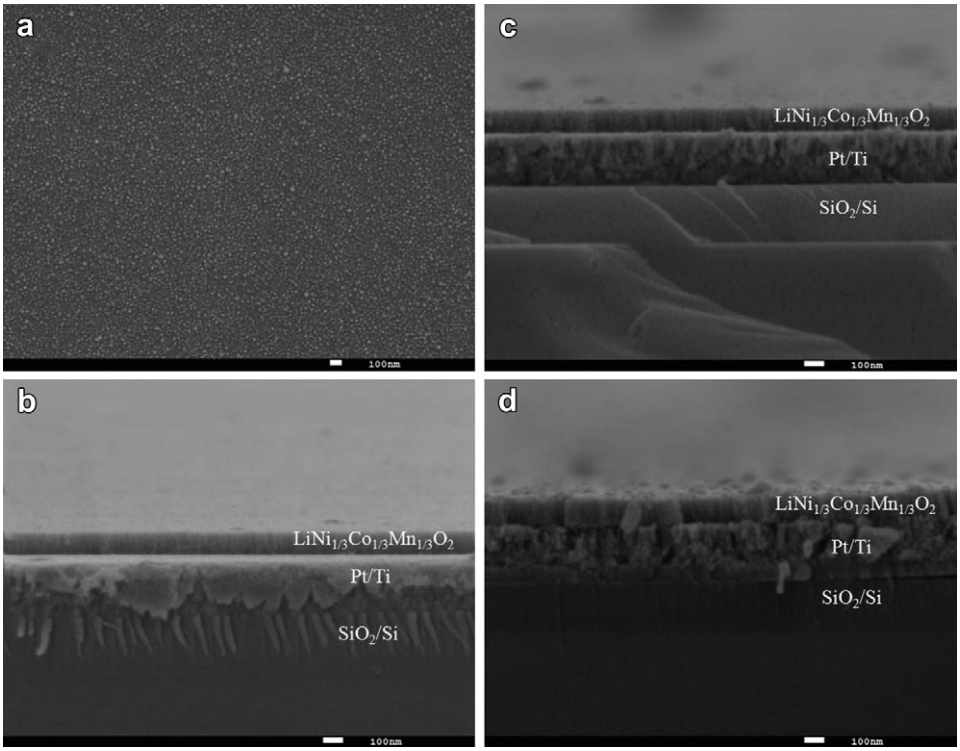

Fig. 3. FE-SEM surface and cross-section images of $LiNi_{1/3}Co_{1/3}Mn_{1/3}O_2$ thin films deposited for 30 min with different annealing temperatures: (a) surface image of the thin film annealed at 450 °C, (b–d) cross-section images of the thin films annealed at 400, 450 and 500 °C, respectively.

deposited for 30 min and annealed at 450 °C are shown in Fig. 4a–c. Four peaks are found in the Ni2p spectra. Two main peaks $Ni2p_{3/2}$ and $Ni2p_{1/2}$ at 853.8 and 871.5 eV are in agreement with those reported for $LiNi_{1/3}Co_{1/3}Mn_{1/3}O_2$ powders [16]. The average oxidation state of Ni in the $LiNi_{1/3}Co_{1/3}Mn_{1/3}O_2$ thin film is divalence because the difference in the binding energy (BE) between $Ni2p_{3/2}$ and $Ni2p_{1/2}$ is approximately 17.5 eV, which is indicative of Ni^{2+} [17]. Two characteristic satellite peaks of Ni^{2+} ions, S1 and S2, are noted in addition to two main peaks $Ni2p_{3/2}$ and $Ni2p_{1/2}$. Such two satellite peaks have also been observed in $LiNi_{1/3}Co_{1/3}Mn_{1/3}O_2$ and $LiNi_{0.4}Co_{0.2}Mn_{0.4}O_2$ powders [16,18].

As shown in Fig. 4b, two sharp peaks $Co2p_{3/2}$ and $Co2p_{1/2}$ are at 779.0 and 794.9 eV, and two satellite peaks are at 784.5 and 801.4 eV in the Co2p spectra. The fit for $Co2p_{3/2}$ spectra gives a BE of 779.0 eV. This value matches well with the BE reported for Co^{3+} (779.0 eV) in $Ni_{1/3}Co_{1/3}Mn_{1/3}OOH$ powders [19] and is close to the BE reported for Co^{3+} (779.5 eV) in $LiNi_{1/3}Co_{1/3}Mn_{1/3}O_2$ powders [20].

In the Mn2p spectra (Fig. 4c), the major peak $Mn2p_{3/2}$ is at 642.3 eV and the minor one $Mn2p_{1/2}$ is at 653.9 eV. The BE for $Mn2p_{3/2}$ spectra is in good agreement with the value reported for Mn^{4+} (642.2 eV) in $LiNi_{1/3}Co_{1/3}Mn_{1/3}O_2$ powders [20]. The present XPS results indicate that the oxidation states of Co and Mn ions in the thin film are expected to be trivalence and tetravalence, respectively.

3.3. Electrochemical performance of $LiNi_{1/3}Co_{1/3}Mn_{1/3}O_2$ thin film electrodes

Fig. 5 shows the second charge–discharge curves and the cycle performance for the $LiNi_{1/3}Co_{1/3}Mn_{1/3}O_2$ thin film electrodes deposited for 30 min with various annealing temperatures. The galvanostatic charge–discharge tests of the $Li/LiNi_{1/3}Co_{1/3}Mn_{1/3}O_2$ cell were carried out at a constant current density of 5 uA cm^2 (0.5C rate, 1C = 180 mA g^{-1}) in the voltage range of 2.8–4.3 V. The electrochemical performance is the best for the thin film electrodes annealed at 450 °C. The thin film electrodes show a couple of defined charge/discharge plateaus about 3.7 V and 3.6 V which

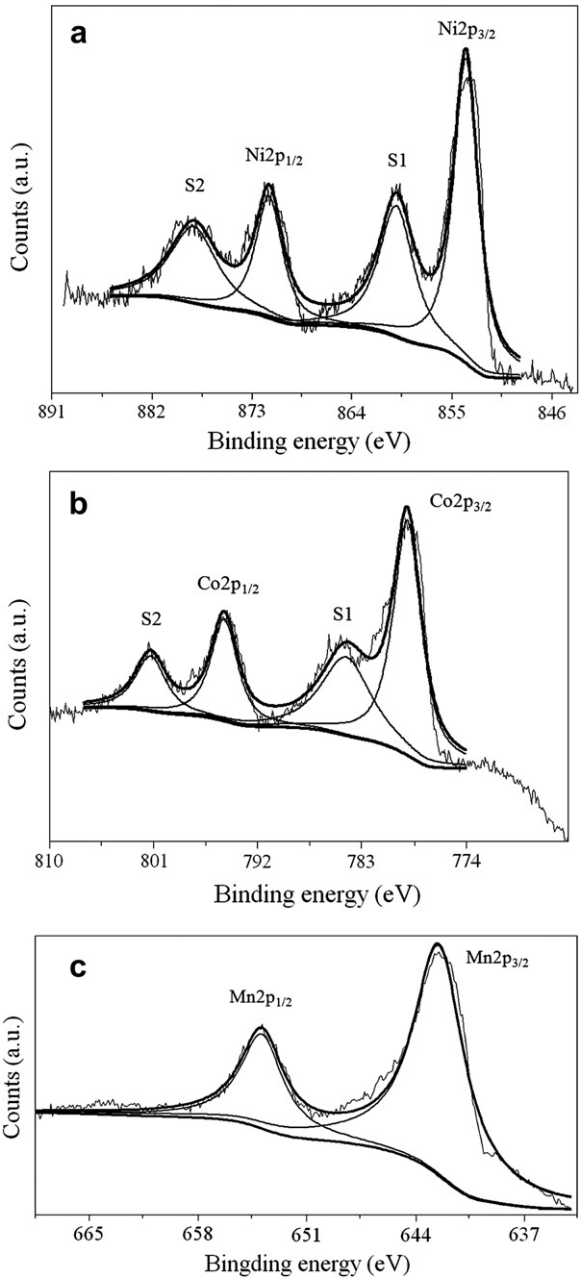

Fig. 4. The Ni2p (a), Co2p (b) and Mn2p (c) XPS spectra of the $LiNi_{1/3}Co_{1/3}Mn_{1/3}O_2$ thin film annealed at 450 °C.

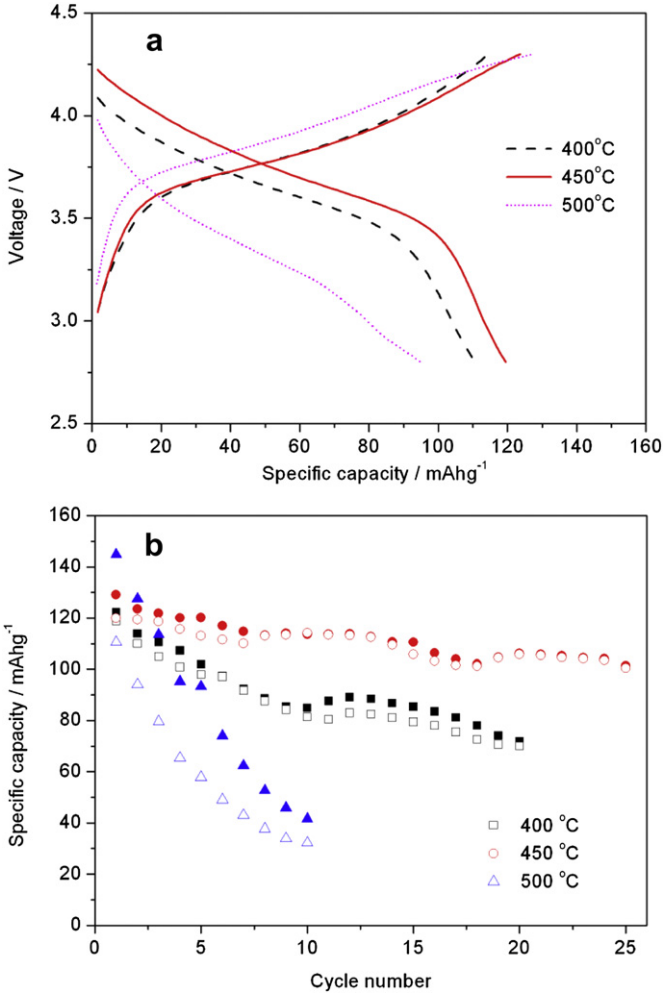

Fig. 5. The charge–discharge curves (a) and cycle performance (b) For the $LiNi_{1/3}Co_{1/3}Mn_{1/3}O_2$ thin film electrodes deposited for 30 min with various annealing temperatures.

corresponds to the deintercalation/intercalation reaction of lithium ions in $LiNi_{1/3}Co_{1/3}Mn_{1/3}O_2$ cathode material. The charge and discharge specific capacities are 123.6 and 119.5 mAh g^{-1}, respectively. The specific capacities were calculated assuming a density of 4.82 gcm^{-3}. It has been reported that the optimal growth temperature is 450 °C for the pulse laser deposited $LiNi_{0.8}Co_{0.15}Al_{0.05}O_2$ film electrodes [21]. The initial specific capacities and coulombic efficiency of the thin film electrodes annealed at 400 °C can be comparable to those of the thin film electrodes annealed at 450 °C. However, the specific capacities decrease fast in the succeeding cycles. The discharge capacity retention ratio is only 59% after 20 charge–discharge cycles. The inferior capacity retention of the thin film electrodes annealed at 400 °C is due to their low crystallinity. When the films are annealed at a low temperature, it is reasonable to expect the thin films have an amorphous structure. Thus, the amorphous $LiNi_{1/3}Co_{1/3}Mn_{1/3}O_2$ may not be stable during Li-ion deintercalation/intercalation and results in a fast capacity fade. The superior electrochemical performance of the thin film electrodes annealed at 450 °C may be ascribed to high crystallinity. Generally, the electrochemical performance in crystalline film is higher than that of amorphous film [22]. In addition, the larger grain size of the thin films annealed at 450 °C leads to the decrease of the grain boundary density, which facilitates the pathway of Li-ion into the thin film.

From Fig. 5b, the specific capacities degrade rapidly for the thin film electrodes annealed at 500 °C. The low cycling stability may be ascribed to poor adhesion strength between the thin films and substrates [23]. The thermal stress induced by the higher annealing temperature may result in poor adhesion strength, then the detachment of the thin films and the loss of electrical contact with the current collectors during cycling. On the other hand, larger grain size may lead to higher mechanical stress during the Li-ion deintercalation and intercalation processes, and thereby result in easy detachment of the thin films from the substrates. Moreover, the larger grain size also can lead to the smaller contact area with the liquid electrolyte, prolong the diffusion distance of the Li^+ ions in $LiNi_{1/3}Co_{1/3}Mn_{1/3}O_2$ thin films and increase the charge-transfer resistance at the electrode/electrolyte interface, which is unfavorable for the charge–discharge cycling stability. The XPS results show a composition of Li in $LiNi_{1/3}Co_{1/3}Mn_{1/3}O_2$ thin films annealed at 500 °C is about 18.8%, indicating the large loss of lithium induced by higher annealing temperature. Li deficiency in the thin films may lead to the formation of impurity phases, which may be one of reasons resulting in low cycling stability of the thin film electrodes. The impurity phases cannot be detected by X-ray diffraction, inferring a small amount of impurity phases.

Fig. 6a shows the charge–discharge curves tested at a constant current density of 5 $uAcm^{-2}$ for the $LiNi_{1/3}Co_{1/3}Mn_{1/3}O_2$ thin film electrodes deposited for 30 min with an annealing temperature of 450 °C. It should be mentioned that the initial open circuit voltage (OCV) was about 3.2 V when the cell was assembled. The initial charge and discharge specific capacities are 130 mAh g^{-1} and 120 mAh g^{-1}, respectively. The discharge specific capacity is comparable to that of the $LiNi_{1/3}Co_{1/3}Mn_{1/3}O_2$ film electrodes prepared by RF magnetron sputtering [14]. The initial discharge specific capacity is about 145 mAh g^{-1} measured between 2.5 V and 4.5 V at a current density of 7.8 μA cm^{-2} (0.24C rate) for the 600 °C-annealed $LiNi_{1/3}Co_{1/3}Mn_{1/3}O_2$ thin films (600 nm) growth on Au substrate. However, it is a pity that the cycle performance of the $LiNi_{1/3}Co_{1/3}Mn_{1/3}O_2$ film electrodes deposited by magnetron sputtering is not reported.

The coulombic efficiency (Fig. 6b) is beyond 95% in addition to the first cycle. This reveals good reversibility of lithium intercalation/deintercalation reactions in the thin film electrodes. The $LiNi_{1/3}Co_{1/3}Mn_{1/3}O_2$ thin film electrodes deliver a good cycle

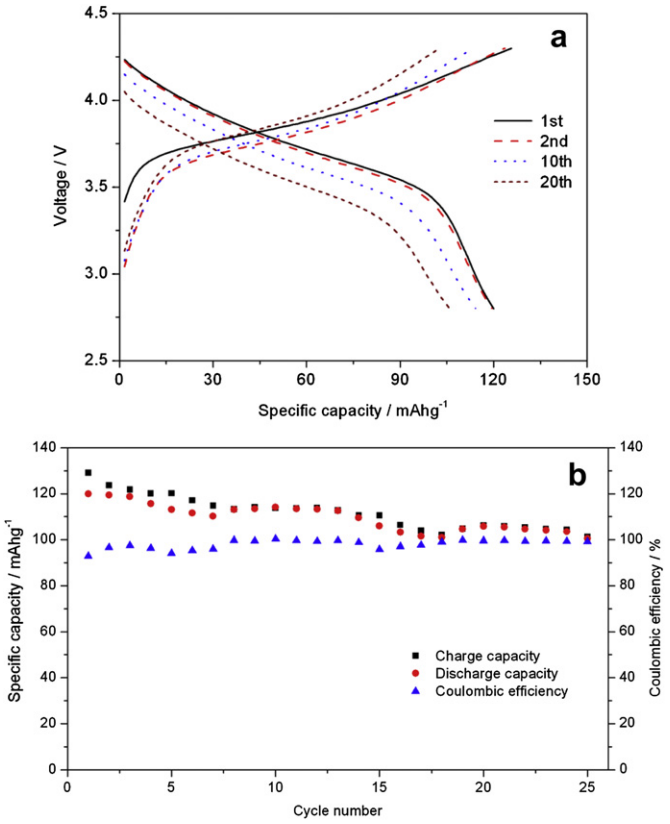

Fig. 6. The charge–discharge curves (a) and coulombic efficiency (b) For the $LiNi_{1/3}Co_{1/3}Mn_{1/3}O_2$ thin film electrodes deposited for 30 min and annealed at 450 °C.

performance, as shown in Fig. 6b. The discharge specific capacity at the 25th cycle is 101 mAh g^{-1}, which is 92% of the initial discharge specific capacity. However, the capacity is low compared with the $LiNi_{1/3}Co_{1/3}Mn_{1/3}O_2$ composite electrode [24]. The low capacity may be attributed to two reasons. One is the uncompleted crystalline $LiNi_{1/3}Co_{1/3}Mn_{1/3}O_2$ thin film (see Fig. 2). Another is that the thin film is free of conducting agent, and the active area for electrochemical reactions is much smaller than that of the composite electrode in the liquid electrolyte.

The electrochemical rate capability was examined by charge–discharge tests between 2.8 V and 4.5 V at different C-rates. Fig. 7 shows the rate capability of the $LiNi_{1/3}Co_{1/3}Mn_{1/3}O_2$ thin film electrodes annealed at 450 °C. The thin films were deposited for 30 and 60 min, respectively. The electrochemical performance of thin film electrodes deposited for 90 min was not tested because the thin films peeled off from the substrates under the annealing temperature of 450 °C for 3 h. The thin film electrodes deposited for 60 min with a thickness of 250 nm show low rate capability and inferior cycle performance, compared to the thin film electrodes deposited for 30 min. From the SEM results, it is confirmed that the grains grow larger and the thin films become thicker with the increase of deposition time. The larger grains make smaller surface area and the fast charge–discharge disable, also can increase the diffusion distance of the Li^+ ions in the thin film electrodes, resulting in low rate capability. In addition, high mechanical stress built up in thick films may also lead to easier detachment of the films from the substrates during the charge/discharge process, thus low capacities and inferior cycle performance.

The thin film electrodes deposited for 30 min deliver good electrochemical performance, including high capacity, good rate capability and cycling stability. The discharge specific capacities

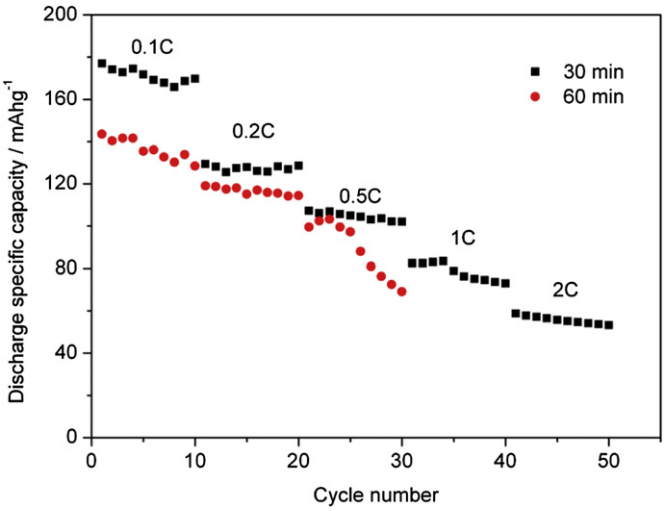

Fig. 7. The rate capability of the $LiNi_{1/3}Co_{1/3}Mn_{1/3}O_2$ thin film electrodes annealed at 450 °C.

of the thin film electrodes at the first cycle and 10th cycle are 177 mAh g^{-1} and 170 mAh g^{-1} at a rate of 0.1C, respectively. The discharge capacities can be comparable to those of the $LiNi_{1/3}Co_{1/3}Mn_{1/3}O_2$ composite electrode [25]. Nevertheless, the thin film electrodes exhibit lower high-rate-discharge (HRD) capability than the $LiNi_{1/3}Co_{1/3}Mn_{1/3}O_2$ composite electrode [26]. This can be ascribed to the fact that the thin films are conducting agent free. The partially amorphous structure and low electronic conductivity (2.5×10^{-7} S cm^{-1} [27]) of the $LiNi_{1/3}Co_{1/3}Mn_{1/3}O_2$ thin film electrodes are also important factors resulting in its low HRD capability.

Cycle voltammetry measurements were performed in the voltage range 2.8–4.5 V at different scan rates. A typical cyclic voltammogram of the $LiNi_{1/3}Co_{1/3}Mn_{1/3}O_2$ thin film electrodes deposited for 30 min and then annealed at 450 °C is shown in Fig. 8a. The curve exhibits a couple of well-defined anodic and cathodic peaks located at about 3.8 V and 3.6 V. This is a typical characteristic attributed to the deintercalation/intercalation process of Li^+ ions in $LiNi_{1/3}Co_{1/3}Mn_{1/3}O_2$ cathode material [28]. Fig. 8b shows the cyclic voltammograms of the thin film electrodes at different scan rates, which reveals good reversible lithium deintercalation and intercalation reactions and fast lithium diffusion in the thin film electrodes.

3.4. Li-ion diffusion coefficients of $LiNi_{1/3}Co_{1/3}Mn_{1/3}O_2$ thin film electrode

To investigate Li diffusivity in $LiNi_{1/3}Co_{1/3}Mn_{1/3}O_2$ thin film electrode, GITT measurements were performed on the cell. Fig. 9a

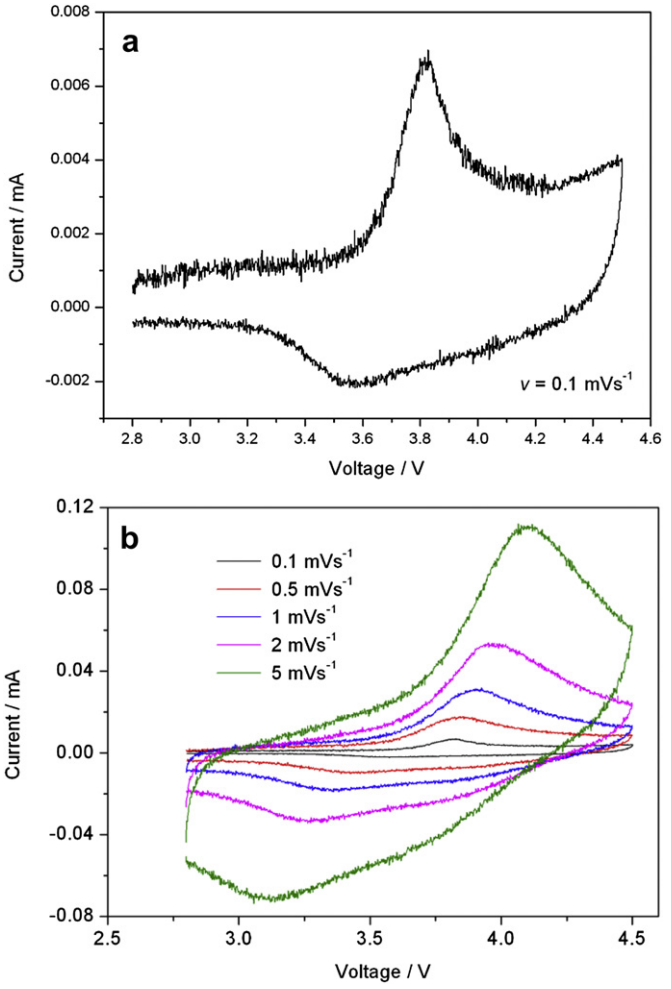

Fig. 8. The cyclic voltammograms of the $LiNi_{1/3}Co_{1/3}Mn_{1/3}O_2$ thin film electrodes deposited for 30 min and annealed at 450 °C: (a) scan rate of 0.1 mV s^{-1} (b) different scan rates.

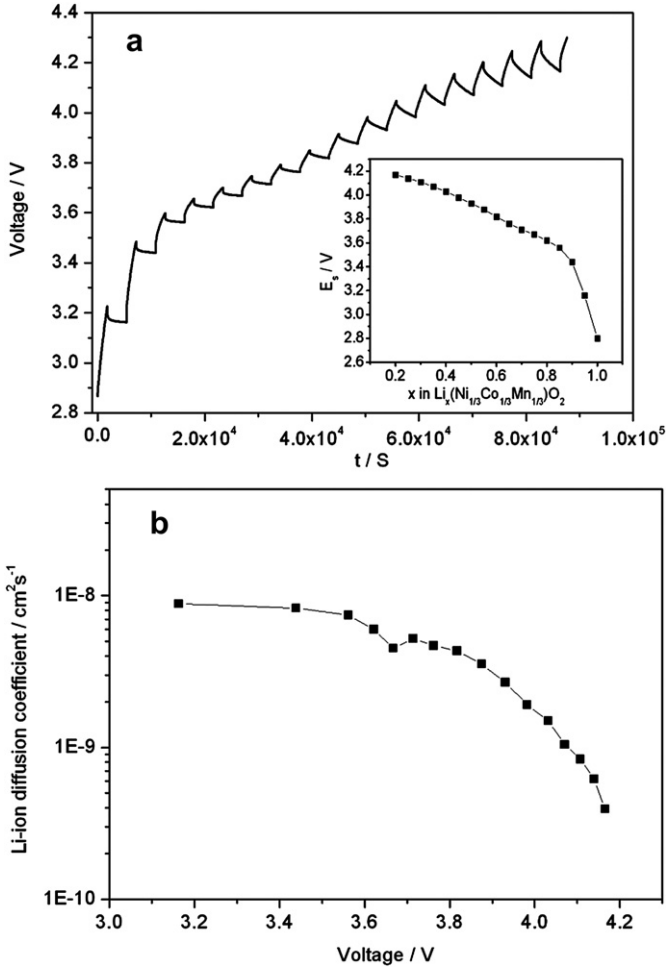

Fig. 9. (a) GITT curve and (b) Li-ion diffusion coefficients of the $LiNi_{1/3}Co_{1/3}Mn_{1/3}O_2$ thin film electrode deposited for 30 min with an annealing temperature of 450 °C. Illustration is the equilibrium voltage E_s as a function of x in $Li_xNi_{1/3}Co_{1/3}Mn_{1/3}O_2$.

shows a typical GITT curve of the $LiNi_{1/3}Co_{1/3}Mn_{1/3}O_2$ thin film electrode deposited for 30 min with an annealing temperature of 450 °C. The GITT measurements were performed by charging the cell for 30 min at a current density of 1 μA cm^{-2}, following by an open circuit relaxation of 1 h to allow the cell voltage to reach its steady-state value. The cell was cycled between 2.8 V and 4.5 V for 5 times prior to the GITT measurements. The equilibrium voltage E_s as a function of x in $Li_xNi_{1/3}Co_{1/3}Mn_{1/3}O_2$ is shown in Fig. 9a (see illustration). The plot of x vs. E_s is very similar to the charge curve in Fig. 6a, which shows a plateau in the range $x = 0.85–0.7$. The cell voltage during the time period τ under an applied constant current density is plotted against $\tau^{1/2}$ which fits into a straight line. Thus, the diffusion coefficients of lithium ions (D_{Li}) in $LiNi_{1/3}Co_{1/3}Mn_{1/3}O_2$ thin film electrode can be determined by Eq. (1) [7]

$$D_{Li} = \frac{4}{\pi\tau}\left(\frac{m_B V_M}{M_B A}\right)^2\left(\frac{\Delta E_s}{\Delta E_\tau}\right) \quad \left(\tau \ll \frac{L^2}{D_{Li}}\right) \tag{1}$$

where D_{Li} ($cm^2\ s^{-1}$) represents the Li-ion diffusion coefficient. m_B (g), M_B (g mol^{-1}), V_M ($cm^3\ mol^{-1}$), A (cm^2) and L (cm) are the mass, molecular weight, molar volume (20.29 $cm^3\ mol^{-1}$), surface area and thickness of the thin film electrode, respectively. ΔE_τ and ΔE_s are the total change of cell voltage (after subtracting the IR drop) and the change of equilibrium voltage for a single titration.

For the film electrode, it is very difficult to determine the mass of the thin film. If we assume that porosity of the film, ε_f, equals to zero, Eq. (1) can be further simplified to Eq. (3) using Eq. (2) [29].

$$V_M/M_B = 1/\rho, \quad m_B = \varepsilon_f \times (\rho \times s \times L) \tag{2}$$

$$D_{Li} = \frac{4}{\pi\tau}L^2\left(\frac{\Delta E_s}{\Delta E_\tau}\right)^2 \quad \left(\tau \ll \frac{L^2}{D_{Li}}\right) \tag{3}$$

In equation (2), ρ is the theoretical density of electrode material. The Li-ion diffusion coefficients, D_{Li}, calculated using Eq. (3) as a function of the cell voltage is shown in Fig. 9b. It is noted that the plot of D_{Li} versus the cell voltage exhibits a minimum around 3.67 V, which coincides with the plateau observed in the voltage profile during charge–discharge cycling. Similar results were also obtained by Shaju [7], Liao [30] and Xia et al. [31]. The values of D_{Li} in $LiNi_{1/3}Co_{1/3}Mn_{1/3}O_2$ thin film electrode are in the range of 10^{-9}–10^{-10} $cm^2\ s^{-1}$. The D_{Li} values in this study are in agreement with the results obtained from GITT in $LiNi_{1/3}Co_{1/3}Mn_{1/3}O_2$ composite electrodes (10^{-9}–10^{-10} $cm^2\ s^{-1}$) [7]. However, the D_{Li} values are higher than those obtained from GITT in 300 °C-annealed $LiCoO_2$ thin films (10^{-12}–10^{-13} $cm^2\ s^{-1}$) [30] and $LiNi_{0.5}Mn_{0.5}O_2$ thin films (10^{-12}–10^{-16} $cm^2\ s^{-1}$) [31].

4. Conclusions

Layered $LiNi_{1/3}Co_{1/3}Mn_{1/3}O_2$ thin film electrodes have been successfully prepared by pulsed laser deposition technique. The microstructure and electrochemical performance of thin film electrodes have been investigated. The electrochemical performance of $LiNi_{1/3}Co_{1/3}Mn_{1/3}O_2$ thin film electrodes depends on the annealing temperature, composition and thickness. The optimum deposition time and annealing temperature are 30 min and 450 °C. The thin film electrodes prepared at the optimum conditions exhibit high capacities, good cycling stability and rate capability. The coulombic efficiency is beyond 95% during cycling tested at 0.5C rate, and the capacity retention ratio is 92% after 25 charge–discharge cycles. The discharge specific capacities at the first cycle and 10th cycle are 177 mAh g^{-1} and 170 mAh g^{-1} tested at 0.1C rate in the voltage range of 2.8–4.5 V, respectively. The Li-ion diffusion coefficients in $LiNi_{1/3}Co_{1/3}Mn_{1/3}O_2$ thin film electrodes are in the range of 10^{-9}–10^{-10} $cm^2\ s^{-1}$ obtained by GITT.

Acknowledgments

This research is jointly supported by the program of Guangxi Natural Science Foundation (Project No. 2012GXNSFBA053154) and the Hong Kong Research Grant Council (RGC) General Research Funds (GRF, No. 9041528).

References

[1] H. Li, Z. Wang, L. Chen, X. Huang, Adv. Mater. 21 (2009) 4593.
[2] W. Tang, L.L. Liu, S. Tian, L. Li, Y.B. Yue, Y.P. Wu, et al., Electrochem. Commun. 12 (2010) 1524.
[3] A. Manthiram, J. Kim, Chem. Mater. 10 (1998) 2895.
[4] D. Belov, M.-H. Yang, J. Solid State Electrochem. 12 (2008) 885.
[5] J.W. Fergus, J. Power Sources 195 (2010) 939.
[6] T. Ohzuku, Y. Makimura, Chem. Lett. 30 (2001) 642.
[7] K.M. Shaju, G.V. Subba Rao, B.V.R. Chowdari, J. Electrochem. Soc. 151 (2004) A1324.
[8] S.-C. Yin, Y.-H. Rho, I. Swainson, L.F. Nazar, Chem. Mater. 18 (2006) 1901.
[9] N. Yabuuchi, Y. Makimura, T. Ohzuku, J. Electrochem. Soc. 154 (2007) A314.
[10] W. Lu, J. Liu, Y.K. Sun, K. Amine, J. Power Sources 167 (2007) 212.
[11] K.M. Shaju, P.G. Bruce, Adv. Mater. 18 (2006) 2330.
[12] Y. Liang, X. Han, X. Zhou, J. Sun, Y. Zhou, Electrochem. Commun. 9 (2007) 965.
[13] F. Zhou, X. Zhao, Z. Lu, J. Jiang, J.R. Dahn, Electrochem. Commun. 10 (2008) 1168.
[14] J. Xie, N. Imanishi, T. Zhang, A. Hirano, Y. Takeda, O. Yamamoto, J. Power Sources 195 (2010) 5780.
[15] C.-H. Lu, Y.-K. Lin, J. Power Sources 189 (2009) 40.
[16] N.V. Kosova, E.T. Devyatkina, V.V. Kaichev, J. Power Sources 174 (2007) 965.
[17] Y.-K. Sun, S.-T. Myung, M.-H. Kim, J. Prakash, K. Amine, J. Am. Chem. Soc. 127 (2005) 13411.
[18] J.-M. Kim, N. Kumagai, T.-H. Chob, J. Electrochem. Soc. 155 (2008) A82.
[19] Z. Chang, Z. Chen, F. Wu, H. Tang, Z. Zhu, X.Z. Yuan, et al., J. Power Sources 185 (2008) 1408.
[20] K.M. Shaju, G.V. Subba Rao, B.V.R. Chowdari, Electrochim. Acta. 48 (2002) 145.
[21] C.V. Ramana, K. Zaghib, C.M. Julien, Appl. Phys. Lett. 90 (2007) 021916.
[22] W.-S. Kim, J. Power Sources 134 (2004) 103.
[23] J.Q. Deng, Z.G. Lu, I. Belharouak, K. Amine, C.Y. Chung, J. Power Sources 193 (2009) 816.
[24] Y. Huang, J. Chen, F. Cheng, W. Wan, W. Liu, H. Zhou, et al., J. Power Sources 195 (2010) 8267.
[25] T.H. Cho, S.M. Park, M. Yoshioa, T. Hiraib, Y. Hideshim, J. Power Sources 142 (2005) 306.
[26] S.K. Martha, H. Sclar, Z.S. Framowitz, D. Kovacheva, N. Saliyski, Y. Gofer, et al., J. Power Sources (2009).
[27] J. Ma, C. Wang, S. Wroblewski, J. Power Sources 164 (2007) 849.
[28] Y.-S. He, Z.-F. Ma, X.-Z. Liao, Y. Jiang, J. Power Sources 163 (2007) 1053.
[29] K.A. Striebel, C.Z. Deng, S.J. Wen, E.J. Cairns, J. Electrochem. Soc. 143 (1996) 1821.
[30] C.-L. Liao, Y.-H. Lee, K.-Z. Fung, J. Alloys Compd. 436 (2007) 303.
[31] H. Xia, Li Lu, M.O. Lai, Electrochim. Acta. 54 (2009) 5986.